The Position Dependence of Strain in Different Regions on Performance of Devices

Yasenjan Ghupur[1, 2], Mamtimin Geni[1], Mamatrishat Mamat[2]
[1]School of Mechanical Engineering, [2]School of Physics Science and Technology, Xinjiang University
[1]Yanan Road 1234, [2]Shengli Road 14, Urumqi, China

Abudukelimu Abudureheman[3]
[3]UMC Japan
Tateyama 294-8502, Japan

***Abstract*--We investigated the position dependence of strain on velocity, current, heat generation rate and resistance in the drain regions for the Si-devices by Monte Carlo simulation method. In this work, we selected ballistic channel Si-diodes with strain in the channel, in the drain and both in the drain and channel regions. The strain treated as a function of Ge contents (x) respectively. The simulation results show the enhancement of the drain current for the case of both strained channel and drain regions is a higher than for strained drain regions, due to the higher in ratio of the velocity of electrons in the drain regions. Moreover, our results show lower in ratios of heat generation rate and resistance in the drain for the both strained channel and drain regions compared to the case of strained drain regions. Our results indicate that the position of strain in the different regions of devices could affect the performance of devices.**

Keywords - Strain, Si-Diode, Ballistic channel, Monte Carlo simulation

I. INTRODUCTION

Further improving the performance of the current semiconductor devices by scaling down the device dimensions brings extremely difficult and technologically challenging problems [1]. Strained-Si (substrate induced strained silicon) recognized as an important method by the International Technology Roadmap for Semiconductors (ITRS) [2], because of its superior transport properties. Recent theoretical research works shown a qualitative agreement with most of the experimental data on strained-Si devices [3, 4]. These studies indicated that applying relaxed $Si_{1-x}Ge_x$ (SiGe, mole fraction x represents the Ge content) as a substrate layer in metal-oxide-semiconductor field-effect transistors (MOSFETs) is one of the most effective ways to introduce larger biaxial tensile strain. The lattice constant of Si being smaller than SiGe creates biaxial tensile strain in the Si [5]. The use of strained-Si channel pseudomorphically grown on a SiGe virtual substrate is becoming a promising way to accelerate the improvement of CMOS performance [6]. About 96% of electrons transporting with small effective mass (m_t, transverse effective mass) are kept in the lowered valleys X_2 (lower in energy), when Ge content (x) in the $Si_{1-x}Ge_x$ reaches 0.15 [6]. When strain causes band splitting, splitting energy between the lowered valleys X_2 (lower in energy) and the raised valleys X_4 (higher in energy) becomes comparable or larger than the optical phonon energy, and this will reduce intervalley scattering [7]. Band splitting results in electrons repopulating from the X_4 valley to the X_2 valley. The repopulation into X_2 causes the average effective mass to decrease and carrier mobility to increase [8]. Using strained-Si for channel and for source and drain have improved p-MOS performance by 20% and 35%, respectively [4, 9].

For short-channel devices, the time for a carrier staying in the channel is greatly reduced and the probability of scattering is decreased [7]. At the room temperature, if channel length is reduced to less than or comparable to the mean free path of carriers [10], the device operation is essentially governed by ballistic transport. Using a novel step/edge technique, the research group in IBM fabricated Si MOSFET with a 20 nm channel length [11]. Simulations also show that as device dimensions shrink to around 30 nm, the carrier transport will become near ballistic [12]. In the case of ballistic transport, electrons injected from source

and flowed into drain become hot electrons. The drain current are significantly reduced by the rebound of hot electrons, because of the effects of the scatterings resulted from the hot electrons [13]. Elastic scattering causes the backward scattering of hot electrons from the drain and substantially degrades the peak of mean velocity of the electrons and the current [14, 15].

Using the self-consistent Monte-Carlo approach to solve the semi classical Boltzmann transport equation is very well suited for getting accurate information for ballistic carrier transport in nanoscale devices at least gate length down to 10 nm [16, 17].

The position dependence of strain in the channel [6-8, 18] or in the drain [19] on the performance of devices were investigated. The dependence of strain in both channel and drain regions on performance of devices have not been studied in detailed. Thus, in this study, we have comparatively investigated the dependence of strain in both channel and drain regions on performance of the ballistic channel device implementing a modified ensemble Monte Carlo (MC) simulation method self-consistently coupled with Poisson's equation [20, 21].

II. SIMULATION METHOD

In this work，the considered length of the source, channel and drain are 100, 20 and 100 nm, respectively, and the diode width is 40 nm for silicon n^+-i-n^+ diode along [100] direction. The temperature is 300 K and doping concentrations of the source and drain are $N_D = 10^{18}$ cm^{-3}. It is assumed that the strained-Si in the channel and drain is grown on a relaxed $Si_{1-x}Ge_x$ substrate and is a function of Ge content *x*. Energy bands were modeled by an analytical non parabolic band with respect to six equivalent X-valleys of bulk silicon [20]. Electrons deal with preferentially occupying the lower energy levels (X_2), when the six-fold degenerate X_6 valleys in Si are split into X_2 valleys and X_4 valleys that resulted by in-plane biaxial-tensile strain [22]. In order to minimize complexity for better isolation and better understanding of the effects of strained-Si, we only considered the ionized impurity scattering, intravalley acoustic phonon scattering, intervalley phonon scattering and impact ionization in the source and drain regions. The formulae of the scattering rates for the ionized impurity, intravalley acoustic, and intervalley phonon scattering are same as given in reference [21]. Assumed electrons do not undergo any scattering in the channel, thus, the channel region is intrinsic and ballistic.

Intravalley acoustic phonon scattering can be treated as elastic scattering at room temperature. Phonon coupling constants, phonon energies and the longitudinal/transverse effective masses of the electrons were assumed to be same as in unstrained Si in scattering rate calculations [23]. For intervalley phonon and intravalley acoustic phonon scatterings, we used the parameters in the references of [24] and [20]. Nonparabolic band provides a reasonable approximation to the density of states (DOS) for the conduction bands of bulk silicon. The approximated DOS determines the scattering rates of ionized impurity and the phonon scattering when electron energy less than 2 eV [13].

Impact ionization is important in the strained-Si because of the band gap reduction. The scattering rate $W_{impact}(k)$ is modeled by using a modified threshold expression [25]:

$$E_{impact}(k) = P[E(k) - E_{th}(x)]^2 \qquad (1)$$

Where E_{th} is empirical threshold energy, E(k) is the carrier's energy and P is a prefactor which determine the softness of the threshold. The threshold energy is 1.11 eV for unstrained-Si.

Moreover, nonparabolic band is a good approximation for electron transport when the voltage of the devices is near or less than the band gap [26]. The nonparabolicity parameter is inversely proportional to the band gap $E_g(x)$ for the biaxial strain, and $E_g(x) = 1.11-0.4x$. The splitting energy between the lowered and the raised valleys is empirically represented by $\Delta E = 0.67x$ [27]. .

The threshold energy is assumed to be proportional to the band gap $E_{th}(x) = 1.18E_g(x)/E_g(0)$ for the strained-Si.

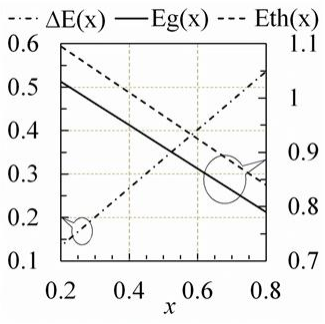

Fig.1 Values of $\Delta E(x)$, $Eg(x)$ and $E_{th}(x)$ with *x*.

Figure 1 shows the values of the band valley splitting $\Delta E(x)$,

the band gap $E_g(x)$ and the threshold energy $E_{th}(x)$ for the strained silicon. The result show that $\Delta E(x)$ linearly increased, whereas $E_g(x)$ and $E_{th}(x)$ linearly decreased with the increasing of the Ge content (x).

For nanoscaled devices, it is necessary to include quantum effects such as in the simulation. In this work, we use this effective potential approach for the modeling of these quantum effects. Since for correcting the quantum effects, an effective potential approach has the advantages of easy numerical implementation and almost guaranteed convergence [28]

The presence of heat generation in the drain extension region is inevitable, and the heat generation has crucial effects on the hot electron transport and the characteristics of nanoscale devices. The drain resistances does not decrease proportional to the channel length [29], but can be estimated using the heat generation [30]. Heat generation rate Q''' [31] and drain resistance R_d [30] are estimated using:

$$Q''' = \frac{N}{N_{\sup} t_{sim} V} \sum \left(h\omega_{ems} - h\omega_{abs} \right) \quad (2)$$

$$R_d = \frac{Q'''}{I_d^2} \quad (3)$$

Where N is the total number of mobile charges in the device, N_{sup} is the number of super particles used in the simulation. (N/N_{sup}) is the scaling ratio of the real Q''' and the simulated Q'''. V is the volume element at each grid node, t_{sim} is the total simulation time, ω_{ems}, ω_{abs} are the emitted and absorbed phonon energy respectively, and I_d is the drain current.

III. RESULTS AND DISCUSSIONS

We selected the range of Ge contents x varying from 0.2 to 0.8 by step 0.05 and the range of drain voltage V_d from 0.2 to 1V by step 0.1, in this work.

The symbols used in the figures such as *ch*, *dr* and *ch&dr* represent a diode with strained channel, with strained drain (sold line) and with simultaneous strained channel and drain (dashed line). The vertical axes of figures are $\Delta A/A = (A_{ij}-A_{cij})/A_{cij}$, where "*A*" represents a value for mean electron velocity (v), current (I_d), heat generation rate (H_d) and resistance (R_d) in the drain regions, respectively. The sub index "*i*" represents the value of applied drain bias voltage (i = 0.2 ~ 1V), j represents Ge content (x), i.e., j = 0.2~0.8, sub index "d" represents the values of "A" in the drain region. A_{cij} represents the case of with strain in the channel (*ch*). The ratios $\Delta v/v$, $\Delta I_d/I_d$, $\Delta H_d/H_d$, $\Delta R_d/R_d$ represent $(v_{ij}-v_{cij})/ v_{cij}$, $(I_{dij}- I_{dcij})/ I_{dcij}$, $(H_{dij} -H_{dcij})/ H_{dcij}$, and $(R_{dij}- R_{dcij})/ R_{dcij}$.

A. Bias voltage dependence of the electron velocity, current, heat generation rate and resistance

In figure 2(a)-(d), the ratio of v, I_d, H_d and R_d in the range of the bias voltage V_d = 0.2~1V for *dr* and *ch&dr* were compared to *ch* for x = 0.4. The figures show ratios of both velocity and current for *ch&dr* are higher, and the ratios of heat generation rate and resistance for *ch&dr* are smaller than the ratios for *dr*.

In the range of V_d = 0.2-0.4 V, the ratios of velocity and current are ~23% and ~20%, the ratios of heat generation rate and resistance change from ~-55% to ~-56% and from ~-65% to ~-69% for *ch&dr*, respectively. In the range of V_d = 0.4-0.6 V, the ratios of velocity and current change from ~24% to ~20% and from ~21% to ~16%, the ratios of heat generation rate and resistance change from ~-60% to ~-50% and from ~-73% to ~-63% for *ch&dr*, respectively. In the range of V_d = 0.6-1 V, the ratios of velocity and current are ~20% and ~16%, the ratios of heat generation rate and resistance ratios are ~-50% and ~-63% for *ch&dr*, respectively. When V_d = ~ 0.5 ~ 1V, the ratio of velocity for *ch&dr* is smaller than for *dr*, and the effect of strain in the channel becomes smaller with the increase of bias voltage

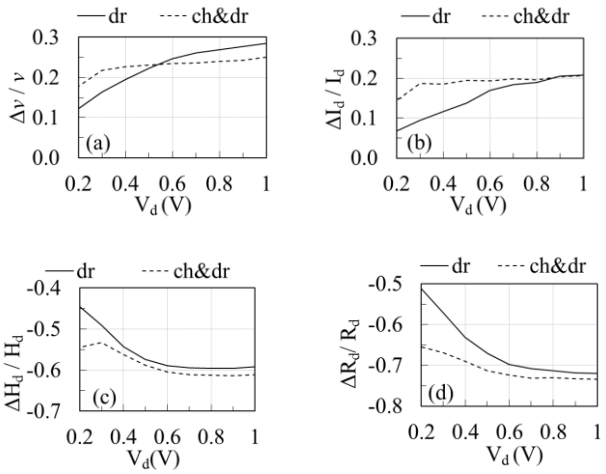

Fig.2 The ratios of velocity (a), current (b), heat generation rate (c) and resistance(d) in the drain region in the range of Vd from 0.2 to 1 V for x = 0.4.

as shown in fig.2 (a) .

B. Strain dependence of the mean velocity, current, heat generation rate and resistance

Fig.3(a)-(d) show ratios of *v*, I_d, H_d and R_d as a function of *x* (from 0.2 to 0.8) when V_d= 0.4 V and for *dr* and *ch&dr*. The figures show ratios of both velocity and current for *ch&dr* are higher and the ratios of heat generation rate and resistance for *ch&dr* are smaller than the ratios for *dr*. In the range of *x* = 0.2-0.3, the ratios of velocity and current are ~24% and the ratios of heat generation rate and resistance change from~-65% to ~-60% and from ~-75% to ~-73% for *ch&dr*, respectively. In the range of *x* = 0.3 ~ 0.6, the ratios of velocity and current change from ~24% to ~20% and from ~21% to ~16%, the ratios of heat generation rate and resistance change from ~-60% to ~-50% and from ~-73% to ~-63% for *ch&dr*, respectively. In the range of *x* = 0.6-0.8, the ratios of velocity and current are ~20% and ~16%, the ratios of heat generation rate and resistance ratios are ~-50% and ~-63% for *ch&dr*, respectively.

Fig.2-3 show the ratios of the drain current and mean velocity in the drain regions for *ch&dr* are higher than the ratios for *dr* as a function of selected Ge content *x* and bias voltages, respectively. Because the number of electrons occupying in the lower energy valleys X_2 is increasing. About 96% of electrons transporting with small effective mass (m_t, transverse effective mass) are kept in the lowered valleys X_2 (lower in energy), when Ge content (*x*) in the $Si_{1-x}Ge_x$ reaches 0.15 [6]. This is due to the effects of simultaneously applied strain in both channel and drain regions is larger than the other cases. For the biaxial tensile strain, when strain causes band splitting, the splitting energy becomes comparable or larger than the optical phonon energy, and this will reduce inter-valley scattering [7]. The reduced intervalley scattering can lower backward scattering of electrons from the drain and reduce the number of hot electrons. Hot electrons readily cause impact ionization and intervalley scattering. If hot electrons experience impact ionization, they will lose their energy and become low energy electrons in the drain. Band splitting results in electrons repopulating from the X_4 (higher in energy) to the X_2 (lower in energy) and thereby most of electrons will locate in the lower X_2 valleys with small m_t. The two effects of strained-Si, the electron transporting with small m_t and the suppressed intervalley scatterings of the electrons can increase the drain current and the mean velocity of electrons. Band splitting results in electrons repopulating from the X_4 valley to the X_2 valley. The repopulation into X_2 causes the average effective mass to decrease and carrier mobility to increase [8].

For strained ballistic channel, the strained-Si results in the increasing of the mean velocity of electrons and the current in the drain region, but could not suppress the intervalley scattering. However, for the strained drain both the electrons transporting with small $m_t$and the suppressed intervalley scattering are play major role. For the strained drain, the strained-Si results in the large increasing of mean velocity of electrons and the current in the drain region due to the two effects of strained-Si. Our study, applying strained-Si both in the channel and drain simultaneously, show a larger increase of the mean velocity and the current in the drain region compared to the case of strained-Si in channel or in drain alone.

Fig.3 (a) - (d) show in the range of *x* = 0.2-0.3, the ratios of velocity and current are higher, the ratios of heat generation rate and resistance changes are lower than the value of ratios at *x*>0.3 for *ch&dr*, respectively. Figure 1 also show the band splitting energy is less than the threshold energy and band gap in the range of 0.2<*x*<0.8. The difference between the splitting energy and the threshold energy and band gap become smaller as a function of *x*. If hot electrons experience impact ionization, they will release

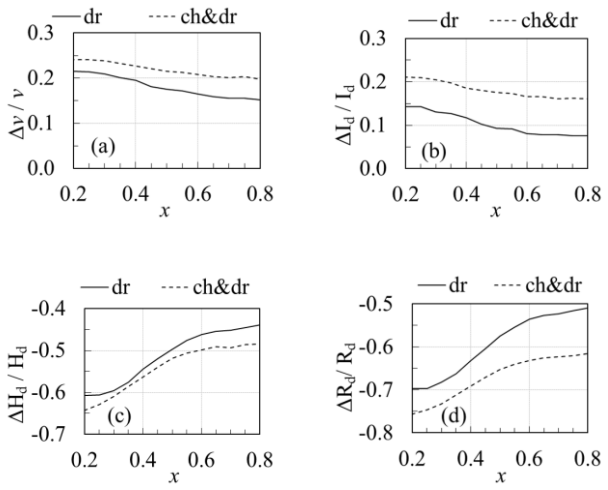

Fig. 3 The ratios of velocity (a), current (b), heat generation rate (c) and resistance (d) in the drain region for ballistic channel diodes with *dr* and *ch&dr*, respectively. The range of the Ge content *x* is 0.2~0.8, when V_d= 0.4 V

their energy and become low energy electrons within drain.

IV. CONCLUSION

We investigated the position dependence of strain on velocity, current, heat generation rate, and resistance in the drain regions for the Si-devices by Monte Carlo simulation method. In this work, we selected ballistic channel Si-diodes with strain in the channel, in the drain and both in the drain and channel regions, as a function of Ge contents (x) respectively. Our results show that the position of strain in the different regions of devices could affect the performance of devices. The enhancement of performance of devices with both strained channel and drain regions is higher than with strained drain or with strained channel regions. The enhancements of performance of devices in the range of x from 0.2 to 0.3 are higher than x greater than 0.3 as figure 3 (a)-(e). The enhancement of the electron velocity and current can be understood as following facts: the electrons transporting with small effective mass (m_t) will locate in the lower X_2-band valleys (lower in energy). The energy of valley splitting which causes the suppressed intervalley scattering is larger than most of the electron's energy. The backward scattering of electrons from drain was lower, thereby increase the mean velocity and drain current in the drain region, because of suppressed intervalley scatterings of electrons. For the strained ballistic channel, the electrons of only those transporting with small effective mass play major role for the increment of electron velocity. In contrast, for the strained-Si in both channel and drain regions, the electrons transporting with small effective mass and the suppressed intervalley scattering play major role for the increment of electron velocity. The results tallies with the report that strain could effectively suppress the inter-valley scatterings of electrons and make electron transporting with small transverse mass [6-8].

ACKNOWLEDGMENT

This work was supported in part by the National Natural Science Foundation of China (Grant No.: 61366001), in part by the National Basic Research Program of China (Grant No.: 2011CB706601), in part by Doctoral fellowship Funding (Grant No.: 208-61344) and in part by New Energy and Industrial Technology Development Organization (NEDO), Japan. Authors are grateful the support and help of Prof. Hiroshi Iwai, Kenji Natori, and associate Prof. Parhat Ahmet at the Tokyo Institute of Technology, Japan. Special thanks to High Performance Computing Platform of Xinjiang University, China.

REFERENCES

[1] W. Yu, B. Zhang, Q.T. Zhao, J.M. Hartmann, D. Buca, A. Nichau, R. Luptak, J.M.J. Lopes, S. Lenk, M. Luysberg, K.K. Bourdelle, X. Wang, S. Mantl, "High mobility compressive strained Si0.5Ge0.5 quantum well p-MOSFETs with higher-k/metal-gate," Solid-State Electron., 62, pp. 185-188, 2011.

[2] ITRS 2010 [http://www.itrs.net/]

[3] O. Bonno, S. Barraud, D. Mariolle, F. Andrieu, "Effect of strain on the electron effective mobility in biaxially strained silicon inversion layers: An experimental and theoretical analysis via atomic force microscopy measurements and Kubo-Greenwood mobility calculations," J. Appl. Phys, 103, pp. 063715, 2008.

[4] P.R. Chidambaram, B.A. Smith, L.H. Hall, H. Bu, S. Chakravarthi, Y. Kim, A.V. Samoilov, A.T. Kim, P.J. Jones, R.B. Irwin, M.J. Kim, A.L.P. Rotondaro, C.F. Machala, D.T. Grider, ieee, "35% drive current improvement from recessed-SiGe drain extensions on 37 nm gate length PMOS," IEEE VLSI Tech. Symp. Dig., pp. 48-49, 2004.

[5] S.E. Thompson, R.S. Chau, T. Ghani, K. Mistry, S. Tyagi, M.T. Bohr, "In search of "forever," continued transistor scaling one new material at a time," IEEE Trans. Semicond. Manuf., 18, pp. 26-36, 2005.

[6] V. Aubry-Fortuna, P. Dollfus, S. Galdin-Retailleau, "Electron effective mobility in strained-Si/Si1-xGex MOS devices using Monte Carlo simulation," Solid-State Electron., 49, pp. 1320-1329, 2005.

[7] S.E. Thompson, G.Y. Sun, Y.S. Choi, T. Nishida, "Uniaxial-process-induced strained-Si: Extending the CMOS roadmap," IEEE Trans. Electron Devices, 53, pp. 1010-1020, 2006.

[8] M. Chu, Y. Sun, U. Aghoram, S.E. Thompson, "Strain: A Solution for Higher Carrier Mobility in Nanoscale MOSFETs," Annu. Rev. Mater. Res, 39, pp. 203–229, 2009.

[9] D.J. Paul, "Silicon germanium heterostructures in electronics: the present and the future," Thin Solid Films, 321, pp. 172-180, 1998.

[10] K. Natori, "Scaling limit of the MOS transistor - A ballistic MOSFET," IEICE Trans. Electron., E84c, pp. 1029-1036, 2001.

[11] A. Hartstein, N.F. Albert, A.A. Bright, S.B. Kaplan, B. Robinson, J.A. Tornello, "A metal-oxide-semiconductor field-effect transistor with a 20-nm channel length," J. Appl. Phys, 68, pp. 2493-2495, 1990.

[12] D.J. Frank, S.E. Laux, M.V. Fischetti, Monte Carlo simulation of a 30 nm dual-gate MOSFET: how short can Si go?, in: IEDM Tech. Dig., Washington, DC, 1992, pp. 553-556.

[13] A. Svizhenko, M.P. Anantram, "Role of scattering in nanotransistors," IEEE Trans. Electron Devices, 50, pp. 1459-1466, 2003.

[14] T. Kurusu, K. Natori, "Numerical study on ballistic n(+)-i-n(+) diode by Monte Carlo simulation: Influence of energy relaxation of hot electrons in drain region on ballistic transport," Jpn. J. Appl. Phys., 45, pp. 1548-1552, 2006.

[15] A. Abudukelimu, W. Yasenjiang, K. Kakushima, P. Ahmet, M. Geni, K. Natori, H. Iwai, "Effects of scattering direction of hot electrons in the drain of ballistic n+-i-n+ diode," Jpn. J. Appl. Phys., 50, pp. 104301-104303, 2011.

[16] P. Palestri, D. Esseni, S. Eminente, C. Fiegna, E. Sangiorgi, L. Selmi, "Understanding quasi-ballistic transport in nano-MOSFETs: Part I - Scattering in the channel, and in the drain," IEEE Trans. Electron Devices, 52, pp. 2727-2735, 2005.

[17] J.S. Martin, A. Bournel, P. Dollfus, "On the ballistic transport in nanometer-scaled DG MOSFETs," IEEE Trans. Electron Devices, 51, pp. 1148-1155, 2004.

[18] A. Karmous, M. Oehme, J. Werner, O. Kirfel, E. Kasper, J. Schulze, "Local strained silicon platform based on differential SiGe/Si epitaxy," J. Cryst. Growth., 324, pp. 154-156, 2011.

[19] A. Abudukelimu, W. Yasenjiang, K. Kakushima, P. Ahmet, M. Geni, K. Natori, H. Iwai, "Influence of strained drain on performance of ballistic channel devices," Semicond. Sci. Technol., 27, pp. 055001, 2012.

[20] C. Jacoboni, L. Reggiani, "The Monte Carlo method for the solution of charge transport in semiconductors with applications to covalent materials," Rev. Mod. Phys., 55, pp. 645-705, 1983.

[21] K. Tomizawa," Numerical Simulation of Submicron Semiconductor Devices ", Artec House, London, 1993.

[22] S. Dhar, H. Kosina, V. Palankovski, S.E. Ungersboeck, S. Selberherr, "Electron mobility model-for strained-Si devices," IEEE Trans. Electron Devices, 52, pp. 527-533, 2005.

[23] T. Maegawa, T. Yamauchi, T. Hara, H. Tsuchiya, M. Ogawa, "Strain Effects on Electronic Bandstructures in Nanoscaled Silicon: From Bulk to Nanowire," IEEE Trans. Electron Devices, 56, pp. 553-559, 2009.

[24] E. Pop, R.W. Dutton, K.E. Goodson, "Analytic band Monte Carlo model for electron transport in Si including acoustic and optical phonon dispersion," J. Appl. Phys, 96, pp. 4998-5005, 2004.

[25] E. Cartier, M.V. Fischetti, E.A. Eklund, F.R. McFeely, "Impact ionization in silicon," Appl. Phys. Lett., 62, pp. 3339-3341, 1993.

[26] M.V. Fischetti, S.E. Laux, "Monte carlo analysis of electron transport in small semiconductor devices including band-structure and space-charge effects," Phys. Rev.B, 38, pp. 9721-9745, 1988.

[27] G. Abstreiter, H. Brugger, T. Wolf, H. Jorke, H.J. Herzog, "Strain-induced two-dimensional electron gas in selectively doped Si/SixGe1-x superlattices," Phys. Rev. Lett., 54, pp. 2441-2444, 1985.

[28] Y.M. Li, T.W. Tang, X.L. Wang, "Modeling of quantum effects for ultrathin oxide MOS structures with an effective potential," IEEE Trans. Nanotechnol., 1, pp. 238-242, 2002.

[29] K. Lee, M. Shur, K.W. Lee, T. Vu, P. Roberts, M. Helix, "A new interpretation of "End" resistance measurements," Electron Device Letters, IEEE, 5, pp. 5-7, 1984.

[30] Y.T. Tsai, T.A. Grotjohn, "Source and drain resistance studies of short-channel MESFETs using two-dimensional device simulators," IEEE Trans. Electron Devices, 37, pp. 775-780, 1990.

[31] E. Pop, S. Sinha, K.E. Goodson, "Heat generation and transport in nanometer-scale transistors," Proc. IEEE, 94, pp. 1587-1601, 2006.